



EFFECTIVENESS EVALUATION OF POSITIVE REINFORCEMENT IN BEAM ELEMENTS OF MOMENT-RESISTANT FRAMES SUBJECTED TO SEISMIC LOADS

V.I. Fernández-Dávila¹ and A.F. López Vergara²

ABSTRACT

The requirement of minimum positive reinforcement in critical sections located at ends of beams of multistory moment-resistant frames according to chapter 21 of the committee ACI 318 building code is evaluated with the aim to determine its behavior due to gravitational and seismic nature loads.

It is noted that the amount of positive reinforcement has direct relation to the capacity of ductility that reinforced concrete sections have to resist negative moments. However, the positive reinforcement has relation to the levels of incursion in the inelastic range, which are not equally distributed according to the level of floor. In accordance with the Park & Ang's damage indices, there is established a greater structural damage concentrated in the lower floor as the minimum requirement of positive reinforcement is increased. In addition, the total damage is greater in the meantime bigger be the amount of minimum positive reinforcement used

Introduction

Several researchers have studied the contribution of compression steel in beams and, from the moment-curvature diagrams ($M - \phi$), it has been determined that increasing the amount of compression steel increases the ductility of the element (Park & Paulay, 1975). This make it possible to make an analogy with the influence of positive reinforcement in the performance of sections requested by negative moments, which are relevant at the ends of beams of moment-resistant frames when are combined seismic (casual) and gravitational (permanent) loads. A priori, the benefit of positive reinforcement in the structural behavior of the ends of beams due to negative moments was identified; however, it is necessary to establish its performance to addressing the seismic phenomenon in full dimension (cyclic loading).

The section 21.3.2.2 of ACI 318 code (ACI, 2005) is analyzed in this study and requires the next: "Positive moment strength at joint face shall be not less than one-half of the negative moment strength provided at that face of the joint". This requirement provides security before not-forecasted seismic loads, but curiously it doesn't have any comment.

¹ Professor of Civil Engineering, Depto. de Estructuras, Universidad Nacional de Ingeniería, Lima. Peru.

² Graduate Student, Escuela de Ingeniería Civil en Obras Civiles, Universidad Central de Chile, Santiago.

Fig. 1 shows the used methodology for this study and included the analysis and seismic design of moment-resistant frames according to the common Chilean structural engineering practice; after this, undergo to a non-linear analysis. Thus, the influence of positive reinforcement in the behavior of studied moment-resistant frames due to simultaneous action of seismic and gravitational loads was analyzed:

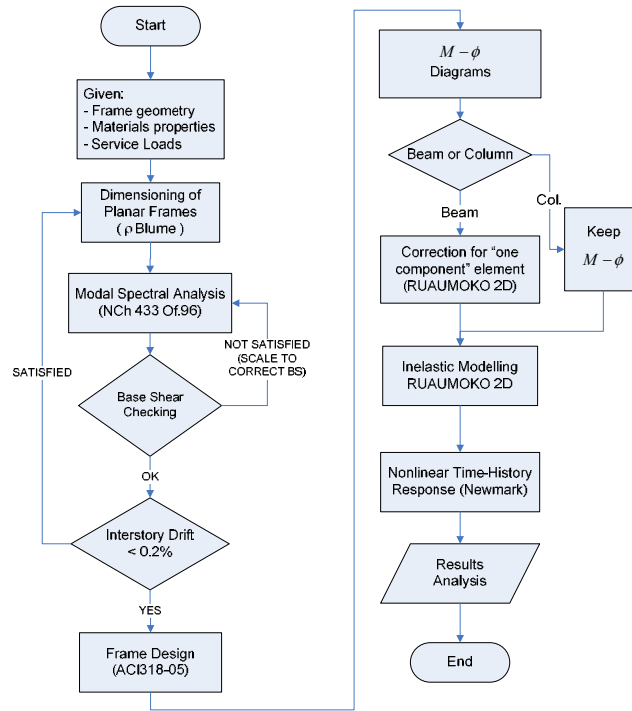


Figure 1. Flowchart of the procedure used.

Structural Models

For the purpose of this study, 3, 5 and 7 story planar moment-resistant frames that can be considered as typical office buildings were designed based on ACI 318-05 with especial emphasis with seismic requirements of Chapter 21. These are characterized by the fundamental period of vibration and are dimensioned so that the value of the period T^* is close to $N/10$, where N is the number of stories.

The material properties of modeled moment-resistant frames are: concrete $f'_c = 25$ MPa and steel with ultimate minimum tension $f_u = 630$ MPa and minimum yield tension $f_y = 420$ MPa. The requirement of minimum strength to positive moments in the critical sections of beams was analyzed varying the steel ratio required for ACI 318. In each moment-resistant frame was evaluated the positive steel ratios $[A_s (+)]$ equals to 25, 50, 75 y 100% of the negative steel ratio located in the ends of the beams and always bigger that the design steel ratio.

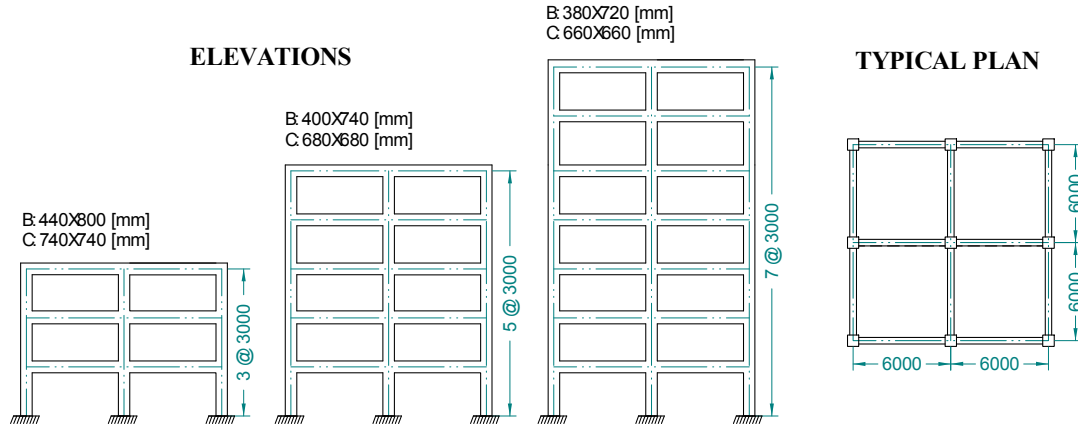


Figure 2. Moment-resistant frame models of analysis.

Loads

For the self-weight of moment-resistant frames it was considered a specific weight equal to $\gamma_h = 2.5 \text{ Ton/m}^3$. Additionally, a gravitational load of 1.5 kPa was added to represent permanent equipments (domestic electrical devices, ceiling, etc.). A value of 2.5 kPa was used to take account of live loads (office buildings)

The seismic loading for the R/C design of frames is carried out through the design spectra defined in the earthquake resistant design code from Chile, NCh 433 (INN, 1996).

Geometric Characteristics

The behavior of the frame due to lateral loads action (seismic) can be characterized by the beam-to-column stiffness ratio ρ (Blume, 1968). It is defined in Eq.1 as the ratio between beams and columns flexural rigidity in the story closest to the midheight of the moment-resistant frame.

$$\rho = \sum \frac{E_b I_b}{L_b} / \sum \frac{E_c I_c}{H_c} \quad (1)$$

Where E , I , L are the elasticity modulus, moment of inertia and length of beams and columns.

The ρ parameter is a measure of the beam restraining to joint rotation and indicates how the moment-resistant frames behaves (Fig. 3). Using $\rho = 1/8$, is possible that beams and columns of the moment-resistant frame has a double curvature deformation (Roehl 1971).

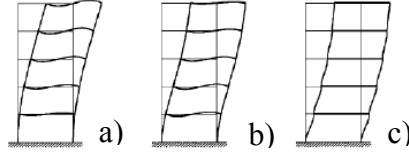


Figure 3. Moment-resistant frame deformation: a) $\rho = 0$; b) $\rho = 1/8$; c) $\rho = \infty$

For the two-bays studied frames, keeping constant $\rho = 1/8$, the elasticity modulus and the relation between bay width and story height, the relation between beams and column sections is:

$$\rho = \sum \frac{E_b I_b}{L_b} / \sum \frac{E_c I_c}{H_c} = \frac{2E I_b}{6E} \frac{H_c}{I_c} \frac{1}{L_b} = \frac{I_b}{3I_c} \frac{1}{2} \Rightarrow \rho = \frac{I_b}{6I_c} \Rightarrow I_c = \frac{4I_b}{3} \quad (2)$$

An analysis as a shear frame (useful in lower frames) and applying static condensation to a stiffness matrix in terms of I_c , the solution of the eigenvalue problem give us the relation with T^* through the value of frequencies. Assuming $T^* = N/10$ we get I_c and then I_b replacing it in Eq.1. This method allows knowing cross sections to get double-curvature behavior in all frames.

Nonlinear Analysis

The inelastic analysis of moment-resistant frames was carried out with the nonlinear analysis software RUAUMOKO 2D (Carr 2006). As seismic load was used the bigger horizontal component measured in the Llo-Lleo's seismographic station during the Chile Central Earthquake (03.03.1985, magnitude 7.8°). The corrected seismic record (N10E) has a maximum acceleration equal to and was scaled to a PGA equal to $0.4 \cdot g$; this value is equivalent to effective acceleration (A_0) for Seismic Zone 3 (INN 1996)

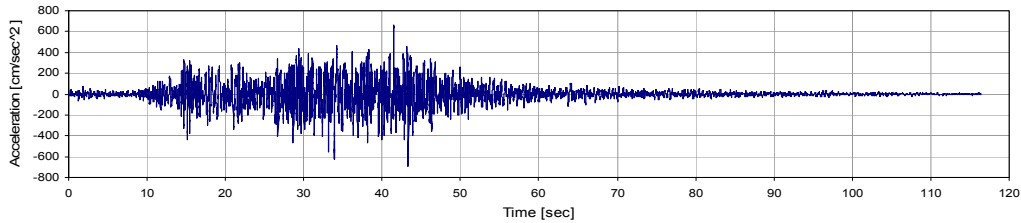


Figure 4. Acceleration record not scaled (Llo-lleo N10E)

The non-linear time history analysis (Newmark 1959) was carried out. For this reason, a value of constant parameter equal to $\beta = 1/4$ and a time step for integration equal to $\Delta t = 0.001$, were considered. For considerer damping action was used the Rayleigh model with tangent stiffness, applying 5% of damping ratio in the first and second vibration modes.

Inelastic Model

Moment-resistant frames models have concentrated plasticity at the ends of elements with a widely used plastic hinge length equal to $l_p = 0.5 \cdot h$, where h is the depth of the beam or

column cross sections.

The inelastic behavior and the ductility in the critical sections of beams and columns were defined through moment-curvature diagrams ($M - \phi$). The frame element (Fig. 5) used for beams and columns in Ruaumoko 2D for the analysis of the inelastic behavior is the "one component" element (Giberson, 1967).

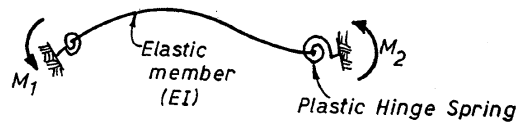


Figure 5. Ruaumoko's element.

The "one component" element only allows the same value for the slopes of $M - \phi$ lines on both ends of elements. This is not congruent with the object of this study. As the area under the $M - \phi$ curve is a good measure of the energy absorption capacity of a R/C section, idealized diagrams (Fig. 6) are used with equivalent area under the curve of real diagrams ensuring the required equality of slopes (Lopez, 2008).

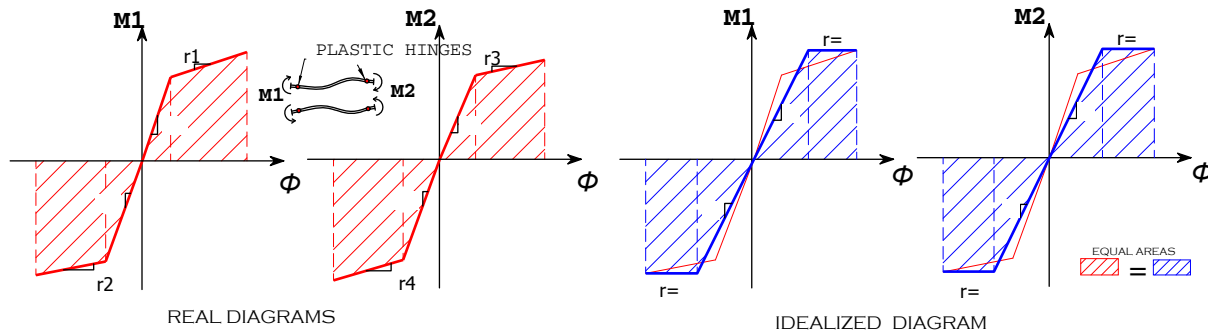


Figure 6. Sketch of changes on moment-curvature diagrams.

Stress-strain relationship

The moment-curvature diagrams ($M - \phi$) were calculated with the modified Kent & Park stress-strain relationship (Park et al 1982), that take account the ductility and strength increase due to concrete confinement. For the steel behavior an elastoplastic model was used and it was amplified the yielding strength in 26% (Malvar, 1998) taking into account the increase of the mechanical properties of steel to the strain velocities to expecting in earthquakes (0.3 sec^{-1}). This value is much higher than the monotonic tests (0.0001 sec^{-1}) to by determining the properties in which are designed the structure.

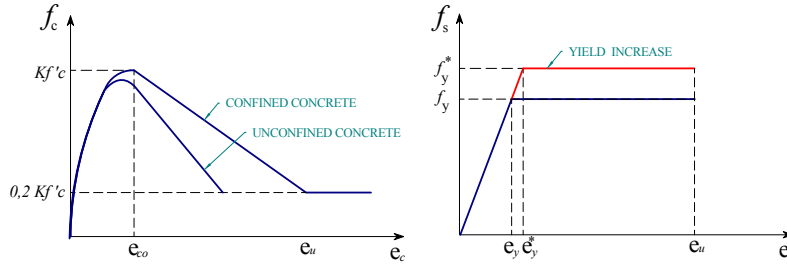


Figure 7. Concrete and steel stress-strain relationships.

Hysteretic behavior

Modified Takeda rule (Otani, 1974) has been used. The Fig. 8 shows the bi-linear hysteretic cycle with parameters that controls the unloading stiffness (α), the reloading stiffness (β) and the loss of stiffness after the yield (r). The analysis includes $\alpha = 0.4$ and $\beta = 0$, both for modeling beams and columns.

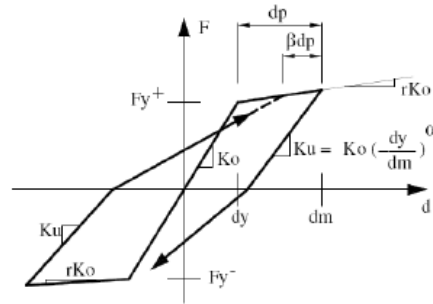


Figure 8. Modified Takeda hysteretic rule (Otani, 1974).

Damage Index

We used the cumulative damage index proposed by Park & Ang (Park et al, 1984). This model combines linearly the maximum damage due to incursion inelastic and the accumulated damage due to the history of deformations.

$$D = \frac{\phi_m}{\phi_u} + \beta_d \frac{\int dE}{M_y \cdot \phi_u} \quad (3)$$

The overall damage indexes are usually obtained as a weighted average of the indexes of local damage. For the weighting was used the criterion to provide greater weight to the most damaged areas, eg weighting functions proportional to dissipated hysteretic energy in the element. This weighting may be performed for each story level as:

$$D_n = \sum (\lambda_i)(D_i) \quad \lambda_i = \left(\frac{E_i}{\sum E_i} \right)_n \quad (4)$$

Where D_n is the total damage of the story n is, λ_i is the weighting of element damage of the story D_i . E_i is the dissipated energy of the element i , and $\sum E_i$ is the sumo of all energy dissipated by the elements of the story i .

In this works was established the relationship of these values with degrees of damage to be expected. Table 1 reproduces the results of the calibration between the observed structural damage in several buildings of reinforced concrete subsequently evaluated the occurrence of earthquakes (Park et al 1986).

Table 1. Intervals measured damage.

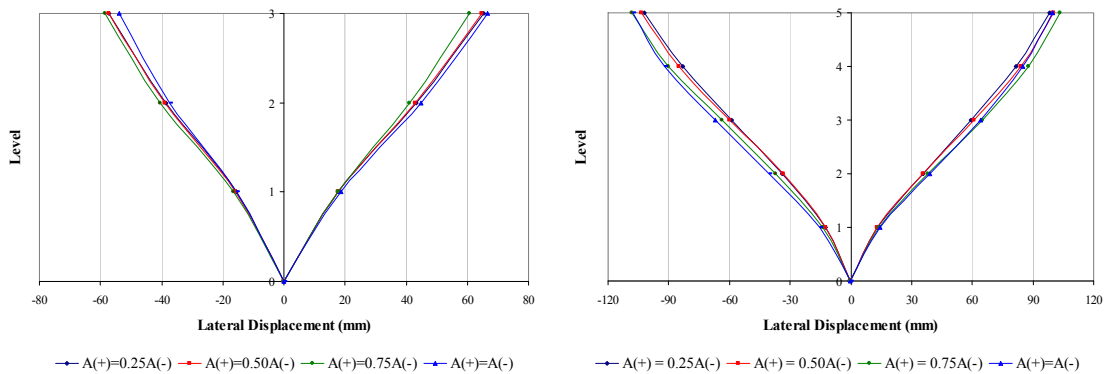
Damage level	No damage	Slight damage	Moderate damage	Severe damage	Collapse
Interval for D	[0, 0.1)	[0.1, 0.2)	[0.2, 0.5)	[0.5, 0.85)	[0.85, 1]

Analysis of the Results

The analysis of results is for the comparison of the performance of the four steel ratios proposed to study the minimum requirement of positive moment reinforcement.

Maximum Lateral Displacements

The analysis of the maximum lateral displacements shows no significant differences due to the influence on the variation of the minimum requirement of positive reinforcement. There is not a clear trend and can be attributed to the numerical dispersion of results.



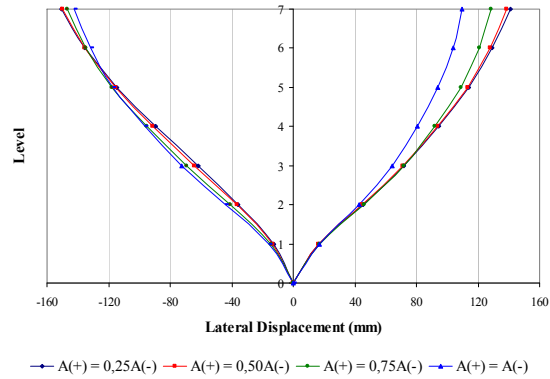


Figure 9. Maximum Lateral Displacements.

Maximum Interstory Drift

It was observed that for all structures the value of the maximum interstory drifts does not vary significantly with the amount of positive reinforcement used. On the upper stories could be seen lower values to drift when increasing positive reinforcement (Fig. 10).

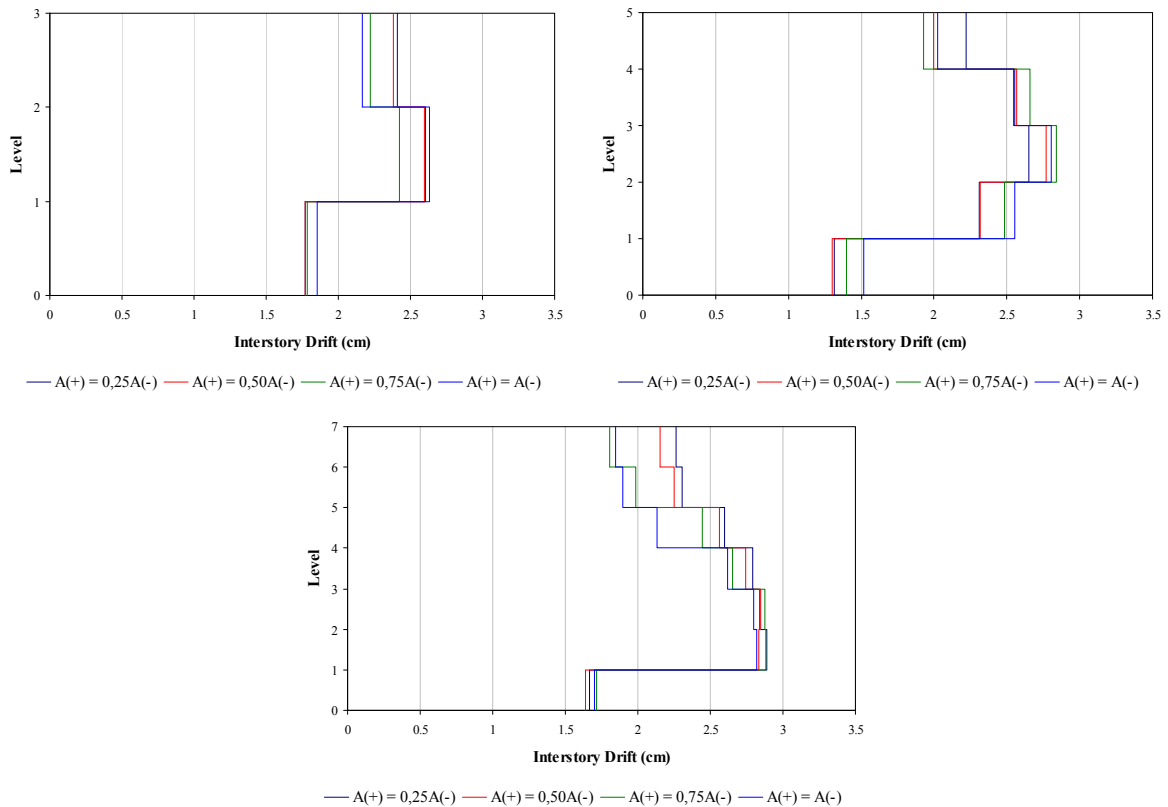


Figure 10. Maximum interstory drifts for the each kind of the moment-resistant frame.

Damage Index

It was observed that increasing the minimum positive reinforcement increases the damage on lower stories, but this does not occur on the upper stories (Fig. 11). For the three-story structure did not show a clear trend and may be due to the development of plastic hinges in columns on the first story, which did not occur in frames 5 and 7 stories. Still, the differences in damage reached in the three-story structures with different positive reinforcement were minimal.

It follows that the maximum damage is concentrated on the lower stories and is directly proportional to the minimum amount needed positive reinforcement. The additional stiffness to positive moment due to the increase of positive reinforcement produces an increase in the negative moments instantly in which the structure is being requested. For this reason, the bigger demand of tension for negative reinforcement and relationship demand vs capacity exceeds expectations in the design stage.

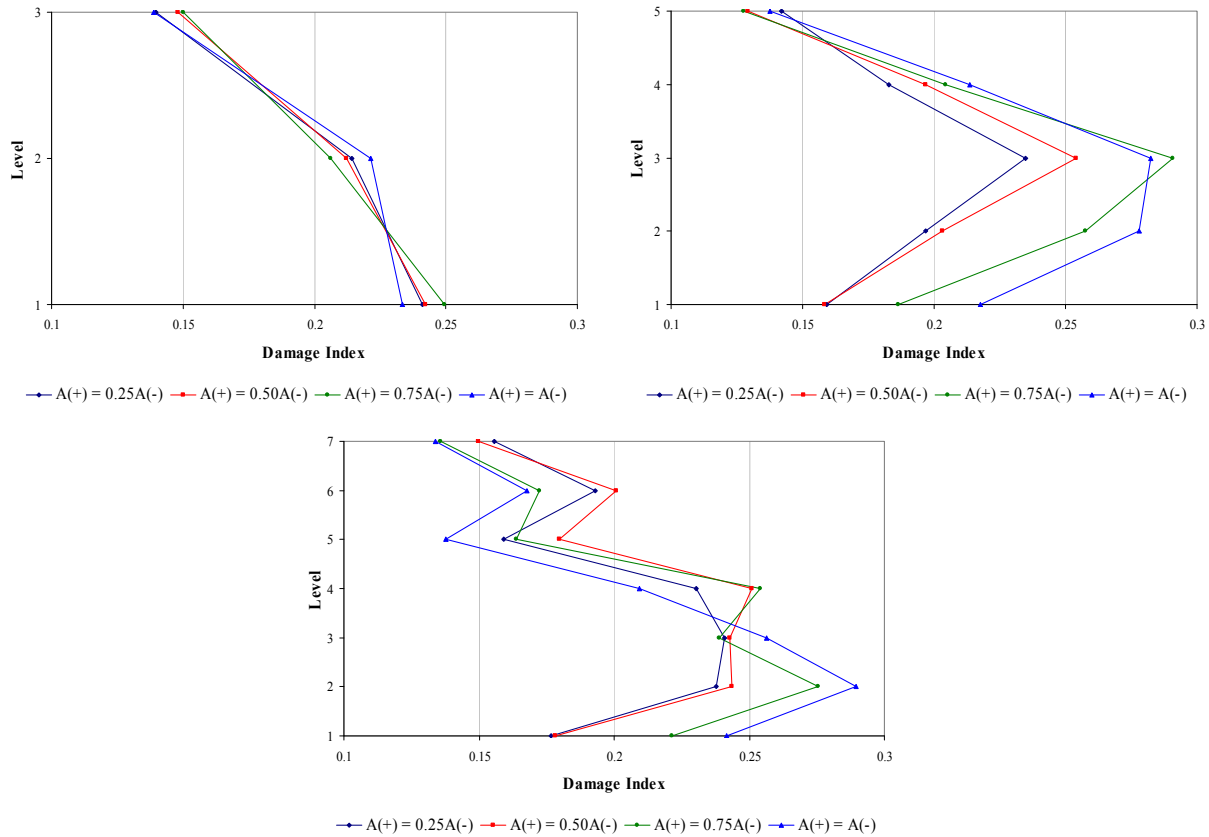


Figure 11. Damage Index

Conclusions

1. Few differences exist in the maximum lateral displacements and the interstorey drifts of the frames, considering minimum values of the steel ratios of positive reinforcement. They do not show a clear trend, and apparently not represent an important parameter.
2. The relationship demand vs capacity, characterized by damage indexes, is vulnerable to

change when vary the value of the steel ratio of positive reinforcement.

3. It was observed that if increase the period of vibration of the frame, there is less amount of damage on the upper stories when increasing positive reinforcement.
4. The increased demand for the damage to the structure is concentrated on one story and is directly proportional to the value of the amount of positive reinforcement.
5. The maximum damage was rated as moderate and does not exceed a severe state, allowing for increased vulnerability to an earthquake of greater intensity.

Acknowledgments

The authors gratefully acknowledge the support for this study provided by the Facultad de Ciencias Físicas y Matemáticas of the Universidad Central de Chile.

References

- ACI American Concrete Institute, 2005. *Building Code Requirements for Structural Concrete and Commentary*, Farmington Hills, Michigan.
- Blume, J.A., 1968. Dynamic Characteristics of Multistory Buildings, *Journal of the Structural Division* (94), 307-402, American Society of Civil Engineers.
- Carr, A.J., 2006. Ruauumoko 2D – The Maori God of Volcanoes and Earthquakes, *Inelastic Finite Element Analysis Program*, Department of Civil Engineering, University of Canterbury, Christchurch, New Zealand.
- Giberson, M.F., 1967. The response of nonlinear multistory structures subjected to earthquake excitation, *Technical Report: CaltechEERL:1967.EERL.1967.002*, California Institute of Technology.
- INN Instituto Nacional de Normalización, 1996. *NCh 433 – Earthquake Resistant Design of Buildings*, Santiago, Chile.
- López, A.F., 2008. Evaluación de la disposición de armadura positiva en secciones críticas de elementos resistentes sometidos a flexión, *Memoria para optar al título de Ingeniero Civil en Obras Civiles*, Universidad Central de Chile, Santiago, Chile. In Spanish.
- Malvar, L.J., Crawford, J.E., 1998. Dynamic Increase Factors for Steel Reinforcing Bars, *Twenty eight DDESB Seminar*, Orlando.
- Newmark, N.M., 1959. Method of Computation for Structural Dynamics, *Journal of the Engineering Mechanics Division* (85), N° EM3, American Society of Civil Engineers.
- Otani, S., 1974. SAKE, A Computer Program for Inelastic Response of R/C Frames to Earthquakes, *Report UILU-Eng-74-2029 Civil Engineering Studies*, University of Illinois, Urbana-Champaign.
- Park, R., Paulay, T., 1975. *Reinforced Concrete Structures*, John Wiley & Sons, New York.
- Park, Y., Ang, A., Wen, Y., 1984. Seismic Damage Analysis and Damage-limiting Design of R/C Buildings, *Technical Report N° SRS 516 Civil Engineering Studies*, University of Illinois, U-C.
- Park, Y., Ang, A., Wen, Y., 1986. Damage-limiting Aseismic Design of Buildings, *Earthquake Spectra*, Earthquake Engineering Research Institute.
- Park, R., Priestley M.J.N., Gill, W.D., 1982. Ductility of Square-confined concrete columns, *Journal of the Structural Division* (108), 929-950, American Society of Civil Engineers.
- Roehl, J.L., 1971. Dynamic Response of Ground-Excited Building Frames, *PhD. Thesis*, Rice University, Houston, Texas.